

# Quantum dark solitons in the one-dimensional Bose gas

Sophie S. Shamailov\* and Joachim Brand†

New Zealand Institute for Advanced Study, Dodd-Walls Centre for Photonics and Quantum Technology,  
Centre for Theoretical Chemistry and Physics, Massey University,  
Private Bag 102904, North Shore, Auckland 0745, New Zealand

(Dated: December 14, 2024)

Dark and grey soliton-like states are shown to emerge from numerically constructed superpositions of translationally-invariant eigenstates of the interacting Bose gas in a toroidal trap. The exact quantum many-body dynamics reveals a density depression with superdiffusive spreading that is absent in the mean-field treatment of solitons. A simple theory based on finite-size bound states of holes with quantum-mechanical center-of-mass motion quantitatively explains the time-evolution of the superposition states and predicts quantum effects that could be observed in ultra-cold gas experiments. The soliton phase step is shown to be a key ingredient of an accurate finite size approximation, which enables us to compare the theory with numerical simulations. The fundamental soliton width, an invariant property of the quantum dark soliton, is shown to deviate from the Gross-Pitaevskii predictions in the interacting regime and vanishes in the Tonks-Girardeau limit.

Dark solitons [1] and related nonlinear wave phenomena are ubiquitous features of superfluids and have been observed frequently in ultra-cold atomic gas experiments [2–9]. The characteristic localised density depression is stabilised by the competing effects of hydrostatic pressure and the stiffness of the superfluid phase. While experiments to date could, for the most part, be well explained by classical wave mechanics, there has been much debate about quantum effects beyond mean-field theory [8, 10–12]. Quantum features of dark solitons are expected to be particularly relevant under reduced dimensionality and in strongly correlated regimes, where quantum fluctuations affect the superfluid phase and destroy long-range coherence. While theoretical works on the one-dimensional Bose gas have predicted effects like greying of the dark soliton [10, 11, 13, 14], and have pointed to a connection of dark solitons to quantum-many-body eigenstates of the Bethe-ansatz solvable Lieb-Liniger model [12, 15–20], the full picture connecting the physical effects with the exact solutions of the model is still missing.

Specifically, Ishikawa and Takayama [16] showed that the dispersion relation of yrast states (eigenstates with lowest energy at given momentum) in the Lieb-Liniger model, known as type-II states, asymptotically approaches that of dark solitons in the Gross-Pitaevskii (GP) or classical nonlinear Schrödinger equation in the high-density limit. However, in contrast to the translationally-invariant yrast states that feature a homogeneous particle density  $N/L$ , classical dark solitons have an inhomogeneous density profile with a characteristic localised dip that propagates with constant velocity. On the other hand, numerical simulations of single-shot measurements of particle position in the yrast states show localised voids appearing at random positions [19, 20].

The situation is better understood for bright solitons, where quantum effects were observed in optics experiments [21, 22] and a full quantum theory could be developed by constructing quantum soliton states as superpositions of translationally invariant eigenstates of an interacting boson model [23–26].

In this Letter we bridge the gap in the quantum theory of dark solitons by constructing quantum states with dark soli-

ton features from superpositions of yrast eigenstates in the form of many-body wave packets. Making use of exact solutions from the Bethe ansatz we simulate the full quantum dynamics. While the expected behaviour of classical dark solitons is found in the high density (weakly interacting) limit, we observe superdiffusion in the crossover to the low-density, strongly-correlated limit, known as the Tonks-Girardeau gas. Modeling the quantum dark soliton as a finite-size quantum mechanical quasiparticle (inspired by Ref. [27]), we identify the velocity, a soliton mass, and a fundamental soliton width as characteristic parameters for the dynamics of the position and width of the simulated density depletion. These parameters are found to be linked back to derivatives of the yrast dispersion relation, for which suitable finite size corrections had to be developed in order to reach quantitative agreement with the numerical simulations. The particle number depletion and a quantity interpreted as the soliton phase step play important roles in the finite size corrections and can also be computed from the dispersion relation.

*Yrast states in the Lieb-Liniger model* – We model a gas of  $N$  bosonic atoms with mass  $m$  in a tightly-confining toroidal trap of circumference  $L$  by the Lieb-Liniger model [28, 29] with repulsive interactions  $c > 0$  [30]

$$\hat{H} = -\frac{\hbar^2}{2m} \sum_{i=1}^N \frac{\partial^2}{\partial x_i^2} + \frac{\hbar^2 c}{m} \sum_{i<j} \delta(x_i - x_j). \quad (1)$$

The eigenstates of  $H$  can be constructed with the Bethe ansatz from the set of  $N$  rapidities  $\{k_j\}$ , which in turn is fully determined by  $N$  quantum numbers  $I_j$  through the Bethe equations

$$k_j + \frac{1}{L} \sum_l 2 \arctan \frac{k_j - k_l}{c} = \frac{2\pi}{L} I_j, \quad (2)$$

where the  $I_j(+\frac{1}{2})$  take integer values for odd (even)  $N$  [31]. While the momentum  $P = \hbar \sum_j k_j = 2\pi\hbar/L \sum_j I_j$  is already determined by the quantum numbers  $I_j$ , the energy  $E = \hbar^2/2m \sum_j k_j^2$  depends on the interaction strength through the rapidities. Of particular relevance are *yrast* states denoted by  $|P, \text{yr}\rangle$ , which are the eigenstates of lowest energy  $E_P^N$  for

given  $P$  and  $N$ . They are found from otherwise contiguous sets of  $I_j$  with a gap of up to one quantum number.

*Quantum dark solitons* – In order to find many-body quantum states that most-closely resemble classical dark solitons, we construct initial states as Gaussian superpositions of yrast eigenstates centered around  $P_0$  with width  $\Delta P$ :

$$|P_0\rangle = \sum_q C_q^{P_0} |q, \text{yr}\rangle, \quad (3)$$

$$C_q^{P_0} = A e^{-\frac{(q-P_0)^2}{4\Delta P^2} + i\frac{qX_0}{\hbar}}, \quad (4)$$

where  $A$  is a normalisation factor and  $X_0$  a displacement. The time evolution is given by  $|P_0(t)\rangle = \exp(-i\hat{H}t/\hbar)|P_0\rangle$ . As the main observable, we construct the single-particle density  $n(x, t)$  from the expectation value of the density operator  $\hat{\rho}(x) = \hat{\psi}^\dagger(x)\hat{\psi}(x)$  as

$$\begin{aligned} n(x, t) &= \langle P_0(t) | \hat{\rho}(x) | P_0(t) \rangle \\ &= \sum_{p, q} C_q^{P_0*} C_p^{P_0} \langle q, \text{yr} | \hat{\rho}(0) | p, \text{yr} \rangle \\ &\quad \times \exp[i(p - q)(x - X_0)/\hbar - i(E_p - E_q)t/\hbar], \end{aligned} \quad (5)$$

where the density form factor  $\langle q, \text{yr} | \hat{\rho}(0) | p, \text{yr} \rangle$  evaluates to a number, which can be calculated from the rapidities  $\{k_j\}$  of the yrast states using formulas derived from the algebraic Bethe ansatz [32–36].

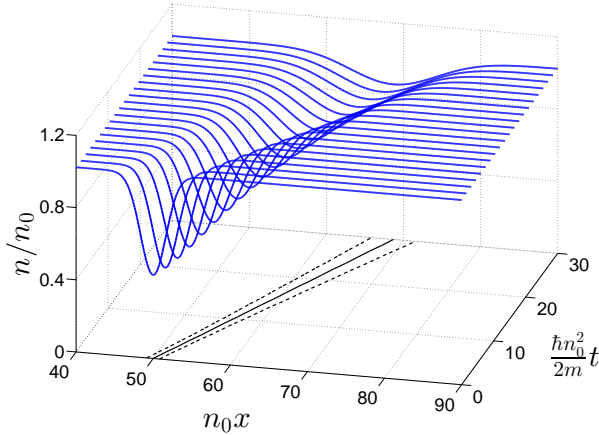


FIG. 1. Time evolution of the quantum dark soliton (3) constructed as a superposition of yrast eigenstates of the Lieb-Liniger model with  $N = 100$  particles at the intermediate interaction strength  $\gamma = 1$ , where  $\gamma = c/n_0$  and  $n_0 = N/L$ . The superposition is prepared with  $\Delta P = 2^{-3/2}\hbar n_0$  and  $P_0 = 2\hbar n_0$ . The solid line tracks the minimum of the dip and the dashed lines on either side of it are displaced by half of the soliton’s width, i.e. by  $\pm\Delta X/2$  [see Eq. (6)].

Figure 1 shows the time evolution of the density profile with initial state (3). Numerical simulations with varying parameters consistently show a smooth and localised density dip that propagates at constant velocity  $v_s$  with  $X(t) = X_0 - v_s t$  while

the width  $\Delta X$  increases over time. Here,  $X \equiv \bar{x}$  measures the position, and the variance of the single particle density measures the width of the dip and is calculated according to

$$\Delta X^2 = \overline{x^2} - \bar{x}^2, \quad (6)$$

where the average  $\bar{A} = \int A \tilde{n} dx / N_d$  is evaluated with respect to the density deviation  $\tilde{n} = n(x) - n_{\text{bg}}$  from the constant background  $n_{\text{bg}}$  [37]. The quantity  $N_d = \int \tilde{n} dx$  measures the particle number depletion. In our time-dependent simulations, the particle number depletion  $N_d$  remains approximately constant over time. Motion at constant velocity and particle number depletion  $N_d$  with expanding width (i.e. “greying of the dark soliton”) are exactly as expected for quantum dark solitons [10, 13, 38–40]. In the following we will parameterise and quantify the motion of the quantum dark soliton.

*Theory of quantum dark solitons* – We aim to formulate a quantitative theory of the observed propagation at constant velocity  $v_s$  and the spreading of the soliton width. In analogy to the case of bright quantum solitons [24, 25] which consist of finite-size bound states of bosons with a quantum mechanical center-of-mass motion, we assume that the variance of the solitonic dip in the single-particle density of a Gaussian superposition state,  $\Delta X^2$ , can be decomposed as

$$\Delta X^2(t) = \sigma_{\text{fs}}^2 + \sigma_{\text{CoM}}^2(t), \quad (7)$$

where  $\sigma_{\text{fs}}^2$  is the variance of the fundamental soliton, which is constant in time and independent of the superposition parameters  $\Delta P$  and  $X_0$  [41]. The center-of-mass variance  $\sigma_{\text{CoM}}^2(t)$  follows the time evolution of a Gaussian wave-packet in the single-particle Schrödinger equation, given by

$$\sigma_{\text{CoM}}^2(t) = \sigma_0^2 \left[ 1 + \left( \frac{\hbar t}{2M\sigma_0^2} \right)^2 \right], \quad (8)$$

where

$$\sigma_0^2 = \frac{\hbar^2}{4\Delta P^2} \quad (9)$$

is the initial variance of the Gaussian wave-packet density in real space and  $M$  is a mass parameter. The quadratic-in-time growth of the variance in Eqs. (7) and (8) is characteristic of the ballistic motion of free quantum quasiparticles and is faster than diffusion [42]. The same effect is expected for bright solitons [24–26].

The three constant parameters – the soliton velocity  $v_s$ , fundamental width  $\sigma_{\text{fs}}$ , and mass  $M$  – completely characterise the motion of the first and second moment of the quantum dark soliton according to Eqs. (7) – (9). We have performed extensive quantum simulations of the density profile with Eq. (5) and found excellent agreement with this model for a wide range of parameters, as shown in Fig. 2 (within the conditions of a large box  $L \gg \Delta X$  and  $\Delta P \ll \pi\hbar n_0$ ). Interpreting quantum dark solitons as quasi-particles in Landau’s sense [27], it is not surprising that the soliton velocity observed in

simulations agrees with the group velocity  $dE/dP$  and the mass parameter  $M$  with the inertial mass  $(d^2E/dP^2)^{-1}$  of the yrast dispersion relation. In order to reach quantitative agreement with our simulations, a continuous model for the dispersion relation of a finite system is needed.

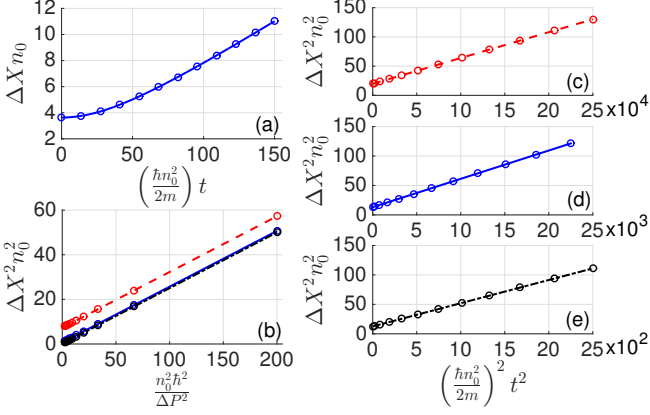


FIG. 2. Width  $\Delta X$  of the density depression from simulations (symbols) compared with fits of Eq. (7) (lines). (a) Ballistic growth of  $\Delta X$  in time for  $\gamma = 1$  with  $\sigma_{fs}$  and  $M$  fitted. (b) Initial variance  $\Delta X^2$  at  $t = 0$  vs.  $\Delta P^{-2}$  used for extracting  $\sigma_{fs}^2$  as the intercept. Interaction strengths  $\gamma = 0.1, 1, 10$  are shown by red dashed, blue continuous and black dotted lines, respectively. Panels (c), (d), (e) show linear fits of  $\Delta X^2$  vs.  $t^2$  used to extract  $M$  for  $\gamma = 0.1, 1, 10$ , respectively, with  $\Delta P = 0.2\hbar m_0/\sqrt{2}$ . All panels used  $P_0 = \pi\hbar m_0$  and  $N = 100$ . The expected quadratic dependence of the variance on  $1/\Delta P$  and  $t$  is evident in all parameter regimes.

*Yrast dispersion relation* – The yrast excitation energy  $E_P^N - E_0^N$  becomes a continuous function  $E_s^\infty(P)$  of momentum in the thermodynamic limit where  $N, L \rightarrow \infty$  while  $n_0 = N/L$  remains constant. The continuous dispersion relation can be obtained by solving Fredholm integral equations [29] and is useful for obtaining various relevant properties for the quasiparticle description as derivatives, e.g. the quasiparticle velocity  $v_s = dE_s^\infty/dP$  and inertial mass  $m_1^{-1} = d^2E_s^\infty/dP^2$ , pertaining to an infinite system. In order to obtain quantitative agreement with our numerical simulations, finite-size corrections need to be applied. The leading  $1/L$  correction terms can be obtained from a conceptually-simple argument based on the assumption that yrast states are associated with (soliton-like) quasiparticles characterised by two features. In particular, these are (a) a particle number depletion  $N_d$  arising from a density dip that is localised on a scale that is small compared to the box size  $L$ , which leads to an elevated background density  $n_{bg} = n_0 - N_d/L > n_0$ , and (b) a nominal ‘‘phase step’’  $\Delta\phi$  that leads to a backflow current with velocity  $v_{cf} = \hbar\Delta\phi/mL$ . The physical picture is that a background current has to flow in order to connect the phase around the ring trap due to periodic boundary conditions. The soliton moving on the background experiences a Galilean boost. The approximate finite system dispersion re-

lation to leading order  $\mathcal{O}(L^{-1})$  is then obtained from

$$E_P^N - E_0^N \approx E_s^N(P) \equiv E_s^\infty(P) + P_s v_{cf} + \frac{1}{2} N m v_{cf}^2 - \frac{N_d^2}{2L} \frac{d\mu}{dn_0}, \quad (10)$$

where  $P_s = N_d m v_s$  is the physical momentum of the moving density depletion and the last term is a correction of the ground state energy due to the localised particle depletion obtained from a Taylor expansion of the equation of state. All quantities on the right hand side of Eq. (10) are evaluated in the thermodynamic limit at the background density  $n_{bg}$ .

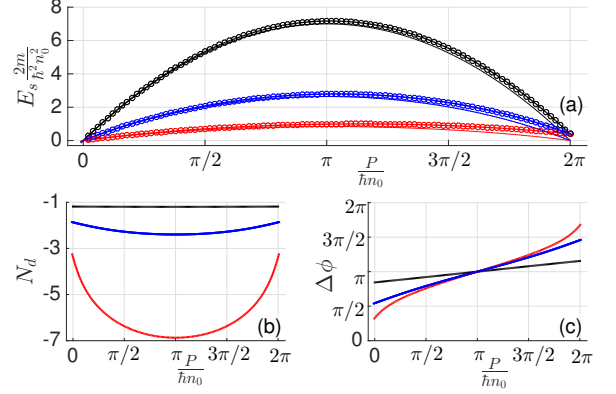


FIG. 3. (a) Dispersion relation of yrast states of the Lieb-Liniger model. Symbols show the excitation energies  $E_P^N - E_0^N$  for  $N = 100$  vs. momentum. Thick lines show the approximate formulae for the finite system (10) and thin lines show the dispersion relations  $E_s^\infty(P)$  in the thermodynamic limit obtained from the Bethe ansatz [29] for comparison. The interaction strengths are  $\gamma = 0.1$  (dashed red line & red circles),  $\gamma = 1$  (full blue line & blue circles), and  $\gamma = 10$  (dash-dotted black line & black circles); the same colour code is used in the bottom panels. Bottom panels: particle number depletion (c) and phase step (d) extracted from the thermodynamic limit dispersion relation with finite size corrections for  $N = 100$ .

The Galilean boost demands that  $P = P_s + N m v_{cf}$ , which can be used to determine the backflow velocity  $v_{cf}$ , and hence the phase step  $\Delta\phi$ , once the particle number depletion  $N_d$  is known. The latter can be computed from the dispersion relation as [43, 44]

$$N_d = - \left( 1 - \frac{v_s^2}{v_c^2} \right)^{-1} \left( \frac{\partial E_s^\infty}{\partial \mu} + \frac{v_s P}{m v_c^2} \right), \quad (11)$$

where the derivative has to be taken at constant  $P$  and  $c, v_c$  is the speed of sound defined by  $m v_c^2 = n_0 d\mu/dn_0$ , and  $\mu = \lim_{N \rightarrow \infty} dE_0^N/dN$  is the chemical potential of the ground state. Equation (11) was derived under similar assumptions to (a) and (b). The dispersion relation is shown in Fig. 3 (a). Both  $N_d$  and  $\Delta\phi$  are shown in the bottom panels of Fig. 3. Finite size corrections to these quantities simply amount to solving the thermodynamic limit Bethe ansatz equations and evaluating  $N_d$  and  $\Delta\phi$  at the elevated background density  $n_{bg}$ .

Even though the assumptions of a localised density dip (a) and a phase step responsible for a superfluid current (b) are

not obviously satisfied for type-II Lieb-Liniger states, we find that the continuous approximation of the dispersion relation is excellent in all interaction regimes as long as  $\sigma_{\text{fs}} \ll L$  [45] (see Fig. 3). In the Tonks-Girardeau limit of  $\gamma \rightarrow \infty$  the approximation (10) becomes exact with  $N_{\text{d}} = -1$ ,  $\Delta\phi = \pi$  and  $E_{\text{s}}^N(P) = [-P^2 + 2Pp_{\text{F}}(1 + N^{-1})]/2m$ , where  $p_{\text{F}} = \pi n_0 \hbar$  is the Fermi momentum. The fact that this approximation works very well implies that the concept of a phase step and a global backflow current is valid in all interaction regimes, despite the fact that global phase coherence should not be expected due to the algebraic off-diagonal long-range order.

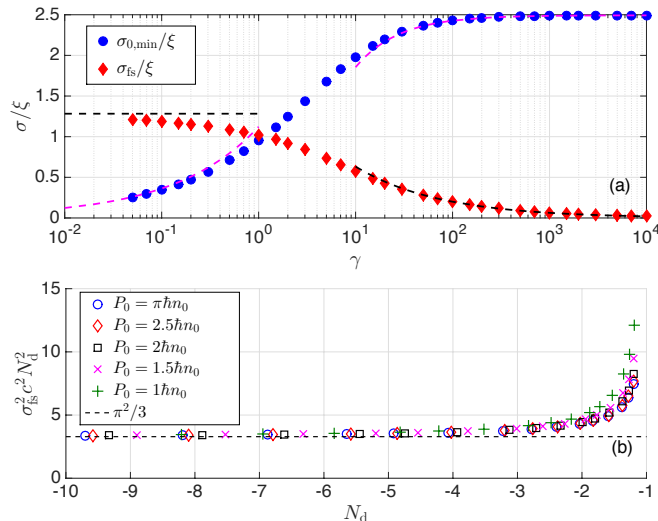


FIG. 4. Length scales of the quantum dark soliton. (a) Fundamental soliton width  $\sigma_{\text{fs}}$  and minimum center-of-mass wave-packet width  $\sigma_{0,\text{min}} \approx 0.8n_0^{-1}$  vs. the coupling strength  $\gamma = c/n_0$  for  $P_0 = \pi\hbar n_0$ . Limiting analytical approximations:  $\sigma_{\text{fs}}/\xi \rightarrow \pi/\sqrt{6}$  from GP theory for  $\gamma \ll 1$  and Eq. (12) for  $\gamma \gg 1$  (black dashed lines). Magenta dashed lines:  $\sigma_{0,\text{min}}/\xi$  with  $\xi \sim 1/(n_0\sqrt{2\gamma})$  for  $\gamma \ll 1$  and  $\xi \sim n_0^{-1}\pi^{-1}(1 + 8/3\gamma)$  for  $\gamma \gg 1$ . (b) Numerical data for the fundamental soliton variance  $\sigma_{\text{fs}}^2$  (multiplied by  $c^2 N_{\text{d}}^2$ ) vs. the particle number depletion  $N_{\text{d}}$  from Eq. (11) (with finite size corrections). Data from different momenta and different coupling strengths collapse onto the same curve and deviate from the result  $\sigma_{\text{GP}}^2$  (dashed line) for the classical dark soliton only near the Tonks-Girardeau limit where  $N_{\text{d}} \rightarrow -1$ . The width  $\sigma_{\text{fs}}$  was extracted from simulation data with  $N = 100$ .

*Length scales* – In contrast to a classical soliton, which propagates with constant shape, the density profile of the quantum dark soliton changes in time. According to Eqs. (7) & (8) the strongest localization occurs at  $t = 0$  and is determined by the fundamental soliton width  $\sigma_{\text{fs}}$  together with the length scale of the Gaussian wave packet  $\sigma_0$ . The choice of the latter is not completely arbitrary but is rather limited by the requirement of  $\Delta P$  fitting in to the fundamental momentum interval  $[0, 2\pi\hbar n_0]$  of the yrast dispersion. We estimate the minimal width of the center-of-mass Gaussian  $\sigma_{0,\text{min}}$  conservatively from Eq. (9) with  $\Delta P \lesssim \pi\hbar n_0/5$ . Figure 4 (a) shows how the two length scales  $\sigma_{\text{fs}}$  and  $\sigma_{0,\text{min}}$  trade their relevance for determining the size limit for the quantum dark

soliton across the crossover from a weakly-interacting Bose gas ( $\gamma \ll 1$ ) to the Tonks-Girardeau gas ( $\gamma \gg 1$ ).

The fundamental soliton width  $\sigma_{\text{fs}}$  is an interesting non-trivial quantity that we extract from numerical simulations by fitting [the procedure is explained in Fig. 2 (b)]. For small  $\gamma$  our data agree very well with the dark soliton width computed from the GP equation according to Eq. (6),  $\sigma_{\text{GP}} = \pi\xi/\sqrt{6(1 - v_{\text{s}}^2/v_{\text{c}}^2)}$ , while for large  $\gamma$ , the fundamental soliton width  $\sigma_{\text{fs}}/\xi$  tends to zero. Close inspection reveals that

$$\sigma_{\text{fs}}/\xi \sim 2/\sqrt{\gamma} \quad \text{for } \gamma \gg 1 \quad (12)$$

fits the numerical data very well [see Fig. 4 (a)]. The vanishing of  $\sigma_{\text{fs}}$  demonstrates that the fundamental soliton changes from a macroscopic object in the GP regime to a single-particle hole without an intrinsic length scale in the Tonks-Girardeau limit.

It is tempting to interpret the quantum dark soliton as a bound state of  $|N_{\text{d}}|$  holes in analogy to quantum bright solitons, which are bound states of  $N$  bosons [24], where the fundamental soliton width is a length scale of the multi-particle bound state [25]. Indeed, the length scale  $\sigma_{\text{GP}}$  for the GP dark soliton can be re-expressed as  $\sigma_{\text{GP}} = \pi/(\sqrt{3}c|N_{\text{d}}^{\text{GP}}|)$ , where the velocity-dependence is fully subsumed in the particle number depletion  $N_{\text{d}}^{\text{GP}}$ . Plotting numerical data for  $\sigma_{\text{fs}}$  vs.  $N_{\text{d}}$  in Fig. 4 demonstrates that data taken at different interaction strengths  $\gamma = c/n_0$  and momenta  $P_0$  falls onto a single curve within numerical accuracy, which means that  $\sigma_{\text{fs}}$  also appears to depend directly only on  $N_{\text{d}}$  and  $c$ . Significant deviations from the GP formula are observed only close to  $N_{\text{d}} = -1$ , which corresponds to the strongly correlated Tonks-Girardeau limit. While these observations suggest that  $\sigma_{\text{fs}}$  may be interpreted as the size of a bound state of  $|N_{\text{d}}|$  holes, it is remarkable that this number is not an integer.

*Conclusions* – The yrast states of the Lieb-Liniger model are strongly correlated, fragmented [18, 46], and contain relevant information about the solitonic dip in high order correlation functions [19]. In this situation it may seem remarkable and surprising that solitonic physics can be extracted and easily quantified by the hypothesized equations (7) – (9). Given that they are well supported by numerical evidence, we may hope that they can eventually be proven within the framework of the Bethe ansatz, and validated by experiments. The significance of the results presented in this Letter, however, goes beyond the specific exactly-solvable model. The emerging picture of quasiparticle dynamics of yrast excitations in a strongly correlated quantum fluid is so simple and physically appealing that we may expect it to be valid for non-integrable systems as well, e.g. ultracold atoms with dipolar interactions, electrons in quantum wires, or Josephson vortices in coupled Bose gases [47].

We thank G. Astrakharchik for discussion. JB thanks the Max Planck Institute for Solid State Research for hospitality during a stay where part of this work was completed. This work was partially supported by the Marsden fund of New Zealand (contract number MAU1604) and by a grant from the Simmons Foundation. This work was performed in part at Aspen Center for Physics, which is supported by National

Science Foundation grant PHY-1607611. SS was supported by the Massey University Doctoral Research Dissemination Grant.

\* [s.shamailov@auckland.ac.nz](mailto:s.shamailov@auckland.ac.nz); Present address: Dodd-Walls Centre for Photonics and Quantum Technology, Department of Physics, University of Auckland, Private Bag 92019, Auckland, New Zealand

† [j.brand@massey.ac.nz](mailto:j.brand@massey.ac.nz)

- [1] Toshio Tsuzuki, “Nonlinear waves in the Pitaevskii-Gross equation,” *J. Low Temp. Phys.* **4**, 441 (1971).
- [2] J. Denschlag, J. E. Simsarian, D. L. Feder, Charles W. Clark, L. A. Collins, J. Cubizolles, L. Deng, E. W. Hagley, K. Helmerston, William P. Reinhardt, S. L. Rolston, B. I. Schneider, and William D. Phillips, “Generating Solitons by Phase Engineering of a Bose-Einstein Condensate,” *Science* **287**, 97–101 (2000).
- [3] S. Burger, K. Bongs, S. Dettmer, W. Ertmer, and K. Sengstock, “Dark Solitons in Bose-Einstein Condensates,” *Phys. Rev. Lett.* **83**, 5198–5201 (1999).
- [4] Naomi Ginsberg, Joachim Brand, and Lene Hau, “Observation of Hybrid Soliton Vortex-Ring Structures in Bose-Einstein Condensates,” *Phys. Rev. Lett.* **94**, 40403 (2005), [arXiv:0408464 \[cond-mat\]](https://arxiv.org/abs/0408464).
- [5] Christoph Becker, Simon Stellmer, Parvis Soltan-Panahi, Sören Dörscher, Mathis Baumert, Eva-Maria Richter, Jochen Kronjäger, Kai Bongs, and Klaus Sengstock, “Oscillations and interactions of dark and dark-bright solitons in Bose-Einstein condensates,” *Nat. Phys.* **4**, 496–501 (2008).
- [6] A. Weller, J. P. Ronzheimer, C. Gross, J. Esteve, M. K. Oberthaler, D. J. Frantzeskakis, G. Theocharis, and P. G. Kevrekidis, “Experimental observation of oscillating and interacting matter wave dark solitons,” *Phys. Rev. Lett.* **101**, 130401 (2008), [arXiv:0803.4352](https://arxiv.org/abs/0803.4352).
- [7] Giacomo Lamporesi, Simone Donadello, Simone Serafini, Franco Dalfovo, and Gabriele Ferrari, “Spontaneous creation of Kibble-Zurek solitons in a Bose-Einstein condensate,” *Nat. Phys.* **9**, 656–660 (2013), [arXiv:1306.4523](https://arxiv.org/abs/1306.4523).
- [8] Tarik Yefsah, Ariel T Sommer, Mark J H Ku, Lawrence W. Cheuk, Wenjie Ji, Waseem S Bakr, and Martin W Zwierlein, “Heavy solitons in a fermionic superfluid,” *Nature* **499**, 426–30 (2013), [arXiv:1302.4736](https://arxiv.org/abs/1302.4736).
- [9] Mark J. H. Ku, Biswaroop Mukherjee, Tarik Yefsah, and Martin W Zwierlein, “Cascade of Solitonic Excitations in a Superfluid Fermi gas: From Planar Solitons to Vortex Rings and Lines,” *Phys. Rev. Lett.* **116**, 045304 (2016), [arXiv:1507.01047](https://arxiv.org/abs/1507.01047).
- [10] J. Dziarmaga, “Quantum dark soliton: Nonperturbative diffusion of phase and position,” *Phys. Rev. A* **70**, 063616 (2004).
- [11] R. Mishmash and L. Carr, “Quantum Entangled Dark Solitons Formed by Ultracold Atoms in Optical Lattices,” *Phys. Rev. Lett.* **103**, 140403 (2009).
- [12] G. E. Astrakharchik and L. P. Pitaevskii, “Lieb’s soliton-like excitations in harmonic trap,” *EPL (Europhysics Lett.)* **102**, 30004 (2012), [arXiv:1210.8337](https://arxiv.org/abs/1210.8337).
- [13] Jacek Dziarmaga and Krzysztof Sacha, “Depletion of the dark soliton: The anomalous mode of the bogoliubov theory,” *Phys. Rev. A* **66**, 043620 (2002).
- [14] Jacek Dziarmaga, Zbyszek P. Karkuszewski, and Krzysztof Sacha, “Quantum depletion of an excited condensate,” *Phys. Rev. A* **66**, 043615 (2002).
- [15] P. P. Kulish, S. V. Manakov, and L. D. Faddeev, “Comparison of the exact quantum and quasiclassical results for a nonlinear Schrödinger equation,” *Theor. Math. Phys.* **28**, 615–620 (1976).
- [16] Masakatsu Ishikawa and Hajime Takayama, “Solitons in a One-Dimensional Bose System with the Repulsive Delta-Function Interaction,” *J. Phys. Soc. Japan* **49**, 1242–1246 (1980).
- [17] R. Kanamoto, L. D. Carr, and M. Ueda, “Metastable quantum phase transitions in a periodic one-dimensional Bose gas. II. Many-body theory,” *Phys. Rev. A* **81**, 023625 (2010), [arXiv:0910.2805](https://arxiv.org/abs/0910.2805).
- [18] Oleksandr Fialko, Marie-Coralie Delattre, Joachim Brand, and Andrey Kolovsky, “Nucleation in Finite Topological Systems During Continuous Metastable Quantum Phase Transitions,” *Phys. Rev. Lett.* **108**, 250402 (2012), [arXiv:1202.5083](https://arxiv.org/abs/1202.5083).
- [19] Andrzej Syrwid and Krzysztof Sacha, “Lieb-Liniger model: Emergence of dark solitons in the course of measurements of particle positions,” *Phys. Rev. A* **92**, 032110 (2015), [arXiv:1505.06586](https://arxiv.org/abs/1505.06586).
- [20] Andrzej Syrwid, Mirosław Brewczyk, Mariusz Gajda, and Krzysztof Sacha, “Single-shot simulations of dynamics of quantum dark solitons,” *Phys. Rev. A* **94**, 023623 (2016), [arXiv:1605.08211](https://arxiv.org/abs/1605.08211).
- [21] M Rosenbluh and R. M. Shelby, “Squeezed optical solitons,” *Phys. Rev. Lett.* **66**, 153–156 (1991).
- [22] P. D. Drummond, R. M. Shelby, S. R. Friberg, and Y. Yamamoto, “Quantum solitons in optical fibres,” *Nature* **365**, 307–313 (1993).
- [23] J. B. McGuire, “Study of Exactly Soluble One-Dimensional N-Body Problems,” *J. Math. Phys.* **5**, 622–636 (1964).
- [24] Y Lai and HA Haus, “Quantum theory of solitons in optical fibers. II. Exact solution,” *Phys. Rev. A* **40**, 854–866 (1989).
- [25] Jayson G. Cosme, Christoph Weiss, and Joachim Brand, “Center-of-mass motion as a sensitive convergence test for variational multimode quantum dynamics,” *Phys. Rev. A* **94**, 043603 (2016), [arXiv:1510.07845](https://arxiv.org/abs/1510.07845).
- [26] Alex Ayet and Joachim Brand, “The single-particle density matrix of a quantum bright soliton from the coordinate Bethe ansatz,” *J. Stat. Mech. Theory Exp.* **2017**, 023103 (2017), [arXiv:1510.04311](https://arxiv.org/abs/1510.04311).
- [27] Vladimir V. Konotop and Lev Pitaevskii, “Landau Dynamics of a Grey Soliton in a Trapped Condensate,” *Phys. Rev. Lett.* **93**, 240403 (2004).
- [28] Elliott H. Lieb and Werner Liniger, “Exact Analysis of an Interacting Bose Gas. I. The General Solution and the Ground State,” *Phys. Rev.* **130**, 1605–1616 (1963).
- [29] Elliott H. Lieb, “Exact Analysis of an Interacting Bose Gas. II. The Excitation Spectrum,” *Phys. Rev.* **130**, 1616–1624 (1963).
- [30] Note that  $c = -2/a_{1D} = gm/\hbar^2$ , where  $a_{1D}$  is the 1D scattering length and  $g$  the effective coupling constant, which can be related to the  $s$ -wave scattering length of ultracold atoms in a tightly confining transverse trap by Ref. [48].
- [31] C. N. Yang and C. P. Yang, “Thermodynamics of a One-Dimensional System of Bosons with Repulsive Delta-Function Interaction,” *J. Math. Phys.* **10**, 1115–1122 (1969).
- [32] N. A. Slavnov, “Calculation of scalar products of wave functions and form factors in the framework of the algebraic Bethe ansatz,” *Theor. Math. Phys.* **79**, 502–508 (1989).
- [33] N. A. Slavnov, “Nonequal-time current correlation function in a one-dimensional Bose gas,” *Theor. Math. Phys.* **82**, 273–282 (1990).
- [34] V. E. Korepin, “Calculation of norms of Bethe wave functions,” *Commun. Math. Phys.* **86**, 391–418 (1982).
- [35] Jean-Sébastien Caux, Pasquale Calabrese, and Nikita A. Slavnov, “One-particle dynamical correlations in the one-

- dimensional Bose gas,” *J. Stat. Mech. Theory Exp.* **2007**, P01008–P01008 (2007).
- [36] Jun Sato, Rina Kanamoto, Eriko Kaminishi, and Tetsuo Deguchi, “Exact relaxation dynamics of a localized many-body state in the 1D Bose gas,” *Phys. Rev. Lett.* **108**, 110401 (2012), [arXiv:1112.4244](#).
- [37] In the numerical procedure  $n_{\text{bg}}$  is evaluated as the maximum value of  $n(x)$ .
- [38] Jacek Dziarmaga and Krzysztof Sacha, “Depletion of the dark soliton: The anomalous mode of the Bogoliubov theory,” *Phys. Rev. A* **66**, 043620 (2002).
- [39] C. K. Law, “Dynamic quantum depletion in phase-imprinted generation of dark solitons,” *Phys. Rev. A* **68**, 015602 (2003).
- [40] R. V. Mishmash, I. Danshita, Charles W. Clark, and L. D. Carr, “Quantum many-body dynamics of dark solitons in optical lattices,” *Phys. Rev. A* **80**, 053612 (2009), [arXiv:0906.4949](#).
- [41] A corresponding result to Eq. (7) was proved in Ref. [25].
- [42] In regular diffusion the growth of the variance is linear in time. The term “quantum diffusion” for quantum solitons that is found in the literature [10] is thus a misnomer.
- [43] M. Schechter, D.M. Gangardt, and A. Kamenev, “Dynamics and Bloch oscillations of mobile impurities in one-dimensional quantum liquids,” *Ann. Phys. (N. Y.)* **327**, 639–670 (2012).
- [44] Sophie S. Shamilov and Joachim Brand, “Dark-soliton-like excitations in the Yang-Gaudin gas of attractively interacting fermions,” *New J. Phys.* **18**, 075004 (2016), [arXiv:1603.04864](#).
- [45] In particular, this condition is typically violated near the edges of the dispersion relation, i.e.  $P_0 \approx 0, 2\pi\hbar n_0$ , and for very weak interactions,  $\gamma \ll 1$ .
- [46] Rafał Ołdziejewski, Wojciech Górecki, Krzysztof Pawłowski, and Kazimierz Rzążewski, “Many-body soliton-like states of the bosonic ideal gas,” (2018), [arXiv:1803.11042](#).
- [47] Sophie S. Shamilov and Joachim Brand, “Quasiparticles of widely tuneable inertial mass: The dispersion relation of atomic Josephson vortices and related solitary waves,” *SciPost Phys.* **4**, 018 (2018), [arXiv:1709.00403](#).
- [48] M Olshanii, “Atomic Scattering in the Presence of an External Confinement and a Gas of Impenetrable Bosons,” *Phys. Rev. Lett.* **81**, 938–941 (1998).